

## ANALYSIS OF STRONG EARTHQUAKE GROUND MOTION FOR PREDICTION OF RESPONSE SPECTRA

MIHAILO D. TRIFUNAC\*

*Earthquake Engineering Research Laboratory, California Institute of Technology, Pasadena, California, U.S.A.*

### SUMMARY

Prediction of response spectra for earthquake engineering purposes is considered from a new point of view based on the dislocation theory of earthquakes. It is shown that the traditional scaling of response spectra by the predicted peak acceleration should be limited to the high-frequency end of the spectrum, and that the peak acceleration in the near field is not strongly correlated with earthquake magnitude. The amplitude of the long-period end of response spectrum at source to station distances greater than about 10 source dimensions should be scaled with seismic moment, while for distances less than about one source dimension this amplitude should be proportional to the permanent ground displacement. To reconcile the existing extensive data on seismicity of active regions based on magnitude scale, it is shown that magnitude can be used to determine approximately the seismic moment.

### INTRODUCTION

Dynamic response of structures to strong earthquake ground motion can be investigated by two different methods. The first method consists of modelling the real structure by a theoretical model<sup>1</sup> and calculating the response for an assumed known motion of the foundation.<sup>2</sup> This approach has recently been used frequently for the final design of important buildings, dams and nuclear power plants. In the other method, also based on idealizing the structure as a mathematical model, the ground motion is represented by its response spectrum and the response is approximated by adding contributions from several modes.<sup>3-6</sup> This method is frequently used for the design of many earthquake-resistant structures, and is the main tool for preliminary design, before the final design can be examined by the first method. In view of the importance of this use of the response spectra for design of earthquake-resistant structures, some basic facts about the physical nature of strong ground motion will be outlined in this paper. Special attention will be given to the basic parameters that link the physical nature of the earthquake source mechanism with the spectral properties of the recorded accelerograms.

For simplicity, the following description of earthquake spectra will focus only on the general and average spectral trends for body waves in an elastic and homogeneous infinite space. Although this simplified characterization is capable of emphasizing the principal physical parameters that govern the nature of strong ground motion and thus provides the basis for semi-empirical correlations between the measured quantities, it must be remembered that the geologic strata between the source and receiver may change the spectral amplitudes appreciably. Analysis of these effects and the study of their influence on the final shape of the response spectra are, of course, beyond the scope of this paper.

Since the introduction of the concept of the response spectrum into earthquake engineering,<sup>3,4</sup> the technique has been refined and improved by many investigators.<sup>5-7</sup> The spectra have been used not only for design, but also in studies of the wave amplification properties of the ground<sup>8</sup> and as a guide in the introduction of dynamic considerations into earthquake-resistant code provisions.

---

\* Assistant Professor of Applied Science.

*Received 2 October 1972*

*Revised 6 March 1973*

The only sound basis for the analysis and prediction of response spectra comes, of course, from the measurement of strong motion. Therefore, Housner in 1959<sup>9</sup> suggested that the idealized velocity spectrum curves, based on the four recorded strong ground motions, be used as 'design spectrum curves'.<sup>10</sup> Since then, numerous investigations have been conducted with the objective of improving the procedures necessary for the prediction of an approximate shape for the scaling of response spectra.<sup>11,12</sup> Although these studies demonstrated that the response spectrum can be characterized by the peak acceleration, peak velocity and peak displacement of ground motion,<sup>11</sup> the relationship between the latter quantities and the earthquake source mechanism received no significant attention. Consequently, in routine design work, the spectral amplitudes are at present still scaled by the peak ground acceleration,<sup>12</sup> which is predicted from the empirical 'relationship' between the earthquake magnitude and the peak acceleration.

The physical characterization of an earthquake by the peak acceleration derived from an earthquake magnitude is very limited indeed. In fact, within the framework of instruments and magnitude definitions<sup>13</sup> currently used, the empirical relationship between peak acceleration and magnitude is usually meaningless. This is because the peak acceleration characterizes the high-frequency end of the spectrum (in the frequency band from about 5 cps to about 20 cps), while the Wood-Anderson and other instruments used in magnitude determinations sample the intermediate and long-period end of the spectrum (say, periods  $T > 1$  sec). In this paper, it will be shown that the overall response spectrum shape can be roughly characterized by the peak acceleration and earthquake magnitude, thus reconciling the important catalogues with this information. According to our new scheme, however, ground acceleration can be used to scale the high-frequency end of the spectrum only, while the magnitude will scale the long-period end.

This paper presents a new rational basis for constructing response spectrum curves when at least two physical parameters describing the source mechanism are available. These parameters are related to the stress in the earthquake source region, the rigidity of rocks, the area of a fault and the average dislocation on the fault surface.

### SIMPLE DISLOCATION MODEL

A simple dislocation model may be represented by a surface  $A$  in an infinite or half-space. To model an earthquake it is usually assumed that the components of displacement become discontinuous across this surface, and the relative displacement on the  $A^+$  surface with respect to the  $A^-$  surface is called the dislocation. During the last decade such models have been successfully used in the interpretation of static deformations observed after earthquakes and in several studies of long-period teleseismic waves.<sup>14</sup> In those studies, however, it was arbitrarily assumed that the dislocation occurs as a step function or a ramp function in time with slope estimated from the expected duration of fault slip. Recently, Brune<sup>14</sup> suggested that the dislocation time function is directly related to the effective stress available to accelerate the two sides of the fault and thus provided a physical basis for understanding the time function and the spectrum at high frequencies. In this theory a simplifying assumption is made allowing for the spontaneous stress drop over the whole fault plane. This assumption is, of course, crude and will have to be abandoned when refinements in theory and measurements become possible, but it seems that, on the average, the velocity of fracture propagation does not affect results much more than other errors inherent in the data processing.

For engineering seismology it is particularly useful to derive simple approximations for the spectra of  $P$  and  $S$  waves.<sup>14,15</sup> Therefore in this paper we will describe a simple dislocation model for  $S$  waves, since such results can be used to improve the methods of response spectrum prediction beyond the capabilities of the present empirical approach.<sup>12</sup> *Mutatis mutandis* in the subsequent expressions, similar results can be derived for  $P$  waves as well.<sup>15</sup>

#### *Near-field S-wave spectra*

An earthquake dislocation might be modelled by a plane surface with area  $A$  located in the infinite space.<sup>14,15</sup> At the time of an earthquake the fracture is accompanied by the displacement discontinuity  $u$  across the dislocation surface resulting from a sudden drop of surface tractions on  $A$ . For simplicity, it can be assumed that the stress pulse produced by this sudden drop of surface tractions is applied instantaneously over the

whole fault surface and that the stress vector lies in  $A$ . The amplitude of the effective stress pulse is then given by  $\sigma = \sigma_0 - \sigma_f$ , where  $\sigma_0$  is the stress before the earthquake and  $\sigma_f$  is the frictional stress acting to resist the fault slip. This stress pulse sends a shear wave propagating perpendicular to the dislocation surface  $A$  (Figure 1). The initial time function for this pulse is

$$\sigma(x, t) = \sigma H(t - x/\beta) \quad (1)$$

where  $H(\cdot)$  is the Heaviside step function,  $t$  is time,  $x$  is distance perpendicular to  $A$  and  $\beta$  is the shear wave velocity.

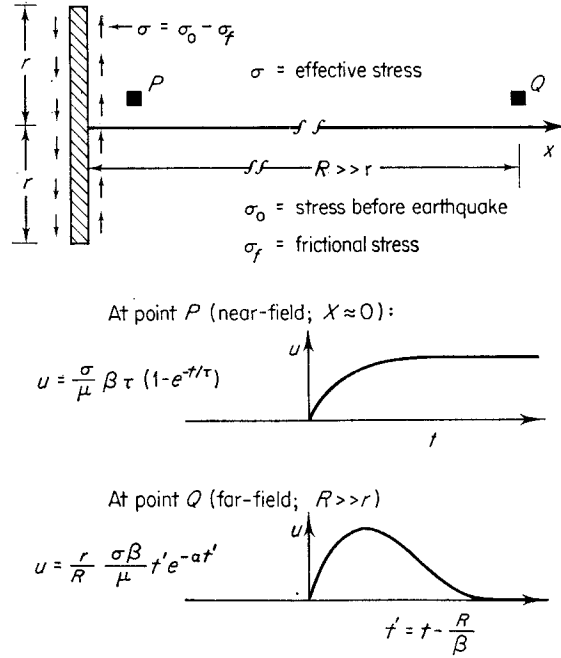


Figure 1. Brune's dislocation model for  $S$  waves

Ground displacement close to the centre of a fault in a direction parallel to the fault motion is obtained by the integration of the one-dimensional wave equation. For the boundary condition at  $x = 0$  (Figure 1) given by

$$\sigma = \mu \frac{\partial u}{\partial x} \quad (2)$$

where  $\mu$  is the Lamé constant, and assuming that  $u = 0$  for  $t \leq 0$ , there follows

$$u = \frac{\sigma \beta}{\mu} t \quad (3)$$

Brune<sup>14</sup> suggested that (3) approximates the first motions on the fault before the effects of fault boundaries reach the point of observation. When that happens the initial particle velocity

$$\dot{u} = \frac{\sigma \beta}{\mu} \quad (4)$$

decreases and gradually approaches zero. This effect can be modelled approximately by

$$\dot{u}(x = 0, t) = \frac{\sigma \beta}{\mu} \exp(-t/\tau) \quad (5)$$

and

$$u(x=0, t) = \frac{\sigma\beta}{\mu} \tau [1 - \exp(-t/\tau)] \quad (6)$$

where  $\tau$  is of the order of  $r/\beta$ .

Note that although (5) and (6) are only approximate representations, they possess two important physical properties. First, the initial velocity is in accordance with (4), i.e. the information about the effective stress  $\sigma$  is preserved. Second, for large  $t$ , (6) tends to a constant level  $\sigma\beta\tau/\mu$ , in agreement with field observations. Thus  $\tau$  can be determined from the known static dislocation amplitude at the point of observation.

The static dislocation caused by an earthquake is, of course, largest near the centre and decreases towards the edges of a fault. This maximum dislocation amplitude can be expressed as

$$u_{\max} = \eta \frac{\sigma r}{\mu} \quad (7)$$

where  $r$  is the characteristic fault-plane dimension and  $\eta$  is a dimensionless parameter depending on the

Table I

Type of faulting and fault geometry	$\eta$	$r$ represents
Dip-slip displacement along an infinitely long narrow strip in a uniform shear field <sup>16</sup>	$\approx \frac{3}{4}$	Fault width
Infinitely long vertical surface fault with strike slip displacement <sup>17</sup>	2	Fault width
Circular fault plane in an infinite medium <sup>18</sup>	$\frac{7\pi}{12}$	Radius of circular dislocation
Elliptical fault plane $x^2/a^2 + y^2/b^2 \leq 1$ ; $\nu$ depends on the ratio $a/b$ , direction of faulting and elastic constants, $1 < \nu < 2$ <sup>19</sup>	$\frac{2}{\nu}$	$r = b$

fault geometry and elastic constants. Several typical values of  $\eta$  ranging from about  $\frac{1}{2}$  to 2 are given in Table I for several simple fault models. From (6) and (7) as  $t \rightarrow \infty$  there follows

$$\tau_{\max} = \eta \frac{r}{\beta} \quad (8)$$

The Fourier amplitude spectrum,  $\Omega_{\text{NF}}(\omega)$ , of the near-field  $S$ -type motion (6) becomes

$$\Omega_{\text{NF}}(\omega) = \frac{\sigma\beta}{\mu} \omega^{-1} (\omega^2 + \tau^{-2})^{-\frac{1}{2}} \quad (9)$$

where  $\omega$  is the circular frequency. Thus (9) implies the acceleration spectrum having a constant amplitude  $\sigma\beta/\mu$  as  $\omega \rightarrow \infty$  and decaying like  $\sigma\beta\tau\omega/\mu$  when  $\omega \rightarrow 0$ , with the transition frequency between these two regions being equal to  $1/\tau$ . Since (9) represents only the first-order approximation for intermediate frequencies, however, it may not represent the true nature of the acceleration spectrum for  $\omega \rightarrow \infty$ . Very high frequencies are rapidly attenuated even for short distances, and the realistic ground accelerations do not have a delta function pulse at  $t = 0$ , as implied by (6); consequently, realistic acceleration spectra decay with increasing  $\omega$ .

#### Far-field $S$ -wave spectra

As the distance to the observation point increases, the static dislocation amplitude decays faster than the dynamic component of motion, and the long wavelength diffraction around the dislocation surface leads to the equivalent source representation by a double couple.<sup>20, 21</sup> To study the average far-field spectrum ( $R \gg r$ ,

Figure 1), Brune<sup>14</sup> proposed to model the *S*-wave ground displacement function with

$$u = \frac{r}{R} \frac{\sigma\beta}{\mu} t' \exp(-\alpha t'), \quad t' \geq 0 \quad (10)$$

where

$$t' = t - R/\beta \quad (11)$$

$r/R$  takes into account the spherical spreading and  $\alpha$ , called the corner frequency of the far-field spectrum, is analogous to  $1/\tau$  in (5) and (6). The Fourier amplitude spectrum of (10) is

$$\Omega_{\text{FF}}(\omega) = \frac{r}{R} \frac{\sigma\beta}{\mu} \frac{1}{\omega^2 + \alpha^2} \quad (12)$$

Apart from the spherical spreading term  $r/R$ , the high-frequency limit of this displacement spectrum is the same as that in (9), while the low-frequency limit leads to the constant

$$\Omega_{\text{FF}}(0) = \frac{r}{R} \frac{\sigma\beta}{\mu} \frac{1}{\alpha^2} \quad (13)$$

It can be shown<sup>22</sup> that the moment  $M_0$  of one couple of a double couple source model is related to the far-field *S*-wave spectrum (13) through

$$\Omega_{\text{FF}}(0) = M_0(4\pi\rho R\beta^3)^{-1} \quad (14)$$

where  $\rho$  is the density of the medium. Since the moment is also given by  $M_0 = \mu\bar{u}A$ ,<sup>23</sup> from (13) and (14) it can be shown<sup>14</sup> that the corner frequency  $\alpha$  becomes

$$\alpha = \left(\frac{7\pi}{4}\right)^{\frac{1}{2}} \frac{\beta}{r} \quad (15)$$

## PARAMETERS DESCRIBING THE SOURCE MECHANISM

A detailed picture of any faulting is undoubtedly given in terms of a highly complicated sequence of events in time and space. The degree to which this complexity can be resolved depends, of course, on the proximity of the available recordings and the frequency band covered by the instrumentation. So far the highest degree of resolution accomplished in source mechanism studies has been through the use of strong-motion accelerograms.<sup>15, 24, 25</sup>

Although many parameters are required to describe fault motion in time and space, strong-motion studies of the source mechanism are, at the present time, mainly concerned only with those parameters that have the most prominent influence on the nature of recorded ground motion. For example, dislocation amplitude, static and dynamic stress drops, the size and shape of a dislocation surface and the velocity at which a dislocation spreads could be considered. In the present elementary approach, however, we will restrict our attention only to the two independent parameters: (1) effective stress  $\sigma$  and (2) the seismic moment  $M_0$ .

The seismic moment  $M_0 = \mu\bar{u}A$ <sup>23</sup> combines information on the rigidity in the source region, average dislocation and the area of faulting in one parameter. The significance of seismic moment emerges from the fact that it specifies the amplitude of the long-period level of the Fourier amplitude spectra of ground motion according to (14) for the far-field spectra and through

$$\bar{\tau} = \frac{M_0}{A\sigma\beta} \quad (16)$$

for the near-field spectra, where  $\bar{\tau}$  is the average of  $\tau$  over the fault plane. Substitution of (16) into (9) gives

$$\Omega_{\text{NF}}(\omega) \approx \frac{\bar{u}}{\omega}, \quad \omega \rightarrow 0 \quad (17)$$

Thus, the information on the overall fault size  $A$  loses its significance near the fault, and the average dislocation becomes the only dominant factor for the long-period components of the near-field Fourier amplitude spectrum. At the fault surface, of course,  $\bar{u}$  in (17) should be replaced by  $u$  at the point of observation.

The effective stress  $\sigma = \sigma_0 - \sigma_f$  is the principal parameter specifying the spectral amplitudes at high frequencies. As  $\omega \rightarrow \infty$  (9) and (12) become

$$\Omega_{\text{NF}}(\omega) \approx \frac{\sigma\beta}{\mu\omega^2}, \quad \omega \gg \frac{1}{\tau} \quad (18)$$

and

$$\Omega_{\text{FF}}(\omega) \approx \frac{r}{R} \frac{\sigma\beta}{\mu\omega^2}, \quad \omega \gg \alpha \quad (19)$$

respectively. Although (18) and (19) imply that the acceleration spectra of  $S$ -waves would have constant amplitudes for high frequencies, attenuation and scattering reduce the observed amplitudes significantly.

The precise nature of attenuation of high-frequency seismic waves (say, for frequencies  $> 1$  cps) is not well understood, partly because of the sparsity of recorded accelerograms. It may be assumed for the purpose of this qualitative discussion, however, that the attenuation of seismic body waves is described by  $2 \exp(-\omega R/2Q\beta)$ , where the  $Q$  factor may range from about 50 to 500,<sup>15, 25</sup> and two models the amplification due to the half-space boundary.

The corner frequencies  $\alpha$  and  $1/\tau$  represent the borderlines between the high- and low-frequency regions of the Fourier amplitude spectra (9) and (12). Their significance lies in their relation to the source dimension  $r$  through (8) and (15). In source mechanism studies based on this simplified theory, source dimensions are inferred from the corner frequencies that are estimated from the spectra of the recorded accelerograms.<sup>15, 25</sup>

## CHARACTERIZATION OF EARTHQUAKE RESPONSE SPECTRA

The Fourier amplitude spectrum not only shows the frequency content of recorded ground motion, but the system response can also be calculated from it.<sup>6</sup> Although the response spectrum has been preferred for structural design purposes, a close relationship between the Fourier amplitude spectrum and the undamped relative velocity response spectrum<sup>6</sup> makes the two essentially interchangeable. We will therefore discuss the physical characterization of Fourier spectra in the subsequent analysis with an understanding that the results apply almost directly to relative velocity spectra as well.

It was shown in the previous sections that Fourier amplitude spectra of strong ground motion may be approximately characterized by only two parameters,  $\sigma$  and  $M_0$ . While it should be clear that such characterization represents only a first-order approximation depicting only general spectral trends, more refined dislocation models will merely introduce additional parameters further describing the spectral amplitudes locally, but they will not significantly alter the trends specified by  $\sigma$  and  $M_0$ . Thus the amplitudes of the high-frequency end of the acceleration spectrum will be determined by the effective stress level  $\sigma$  and the nature of wave scattering and attenuation (Figure 2), while the long-period end of the spectrum will be determined by the seismic moment,  $M_0$ . Of course, the long-period spectral amplitudes are only governed by the static dislocation amplitude  $u$  [equation (17)] for points near a fault. The corner frequency  $\alpha$  or  $1/\tau$ , related to the size of the dislocation surface, determines the frequency at which amplitudes of the long-period end of the acceleration spectrum start falling off. Thus, for a large earthquake associated with long fault fracture and for a fixed level of  $\sigma$ ,  $\alpha$  and/or  $1/\tau$  become small, and the corner period ( $= 2\pi/\alpha$  or  $= 2\pi\tau$ ) increases, augmenting the relative amount of energy present in the long-period waves. The Fourier amplitude spectra in Figure 2 are drawn for the corner period of 10 sec.

For design purposes, the ideal procedure for constructing the Fourier amplitude spectrum of strong-motion acceleration would, therefore, be based on estimates of  $M_0$  and  $\sigma$ .  $M_0 = \mu\bar{u}A$  requires a knowledge of the fault area expected to fracture, average dislocation and the rigidity in the fault region. Although these parameters might be inferred from geologic observations, the rate of slip along the major fault zones, and the length of gaps in seismic activity,<sup>26</sup> estimating the effective stress  $\sigma$  is more difficult.

The traditional approach to the scaling of the response spectrum amplitudes is based on the assumed empirical relationship between peak acceleration and earthquake magnitude.<sup>10,12</sup> Figure 3 summarizes the presently available data on peak acceleration and clearly demonstrates that there is no apparent correlation between peak acceleration and earthquake magnitude. In fact, this figure shows that an earthquake with smaller magnitude can have higher peak acceleration at the same distance. On the other hand, the simplified theory in this paper indicates that peak acceleration should be correlated with the effective stress  $\sigma$ . Although at the present time there are only a few estimates of the effective stress  $\sigma$ ,<sup>15, 23, 25, 27</sup> it seems that for a typical

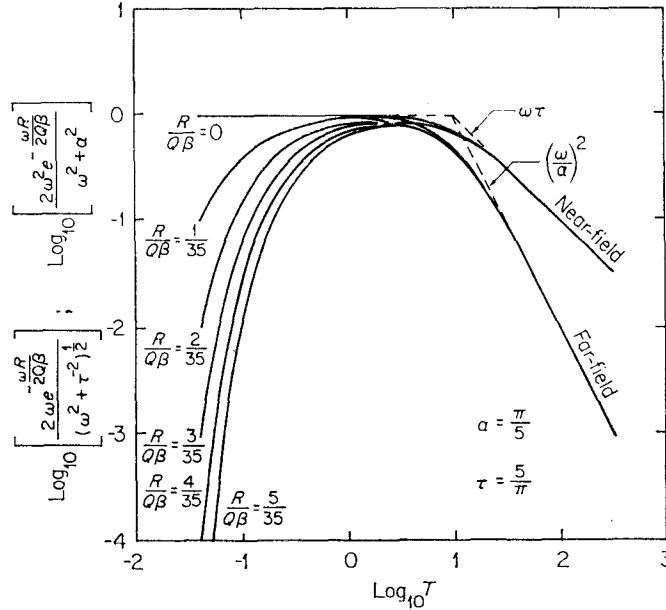


Figure 2. Normalized Fourier amplitude spectra of ground acceleration

earthquake the effective stress averaged over the whole fault plane does not significantly exceed the limit of about 100 bars. This inference is in agreement with the estimate of the average strength of the earth's crust, which is close to several tens of bars.<sup>28</sup> Of course, this does not mean that fracturing in a small region of high stress concentration may not lead to a significantly higher effective stress.<sup>15</sup> Data in Figure 3 suggest that independent of earthquake magnitude, peak acceleration at a given distance may vary by a factor of about 10.

One must know  $\mu$ ,  $\bar{u}$  and  $A$  to scale the long-period end of the spectrum by the moment  $M_0$  for intermediate and large distances ( $R \gg r$ ). Although these quantities might be estimated from the geological and seismological investigations in the area under consideration, frequently the only statistics available are in terms of earthquake magnitude. There are several magnitude scales currently in use, but in this paper we will employ Richter's<sup>13</sup> local magnitude  $M_L$  for shocks less than 6 and the surface wave magnitude<sup>13</sup>  $M_S$  for shocks greater than 6. From equation (14) it is seen that an empirical relationship should exist between the magnitude of an earthquake and the seismic moment  $M_0$ ,<sup>29</sup> since the magnitude gives an estimate of the amplitude of the long-period end of the spectrum if the frequency band of the recording instrument is centred between 0 and  $\alpha$ . Figure 4 presents such a relationship based on data from central and southern California. Although there is an appreciably high scatter of data, a definite trend exists that is given approximately by

$$\log_{10} M_0 = 1.45M + 16.0 \quad (20)$$

where  $M$  stands for  $M_L \leq 6$  or  $M_S \geq 6$ . Therefore, (20) can be used to scale the long-period level of spectra in Figure 2 when the expected earthquake is characterized by the magnitude scale. For the near-field spectra, of course, the static dislocation  $u$  will determine the amplitude of the long-period end of the spectrum.

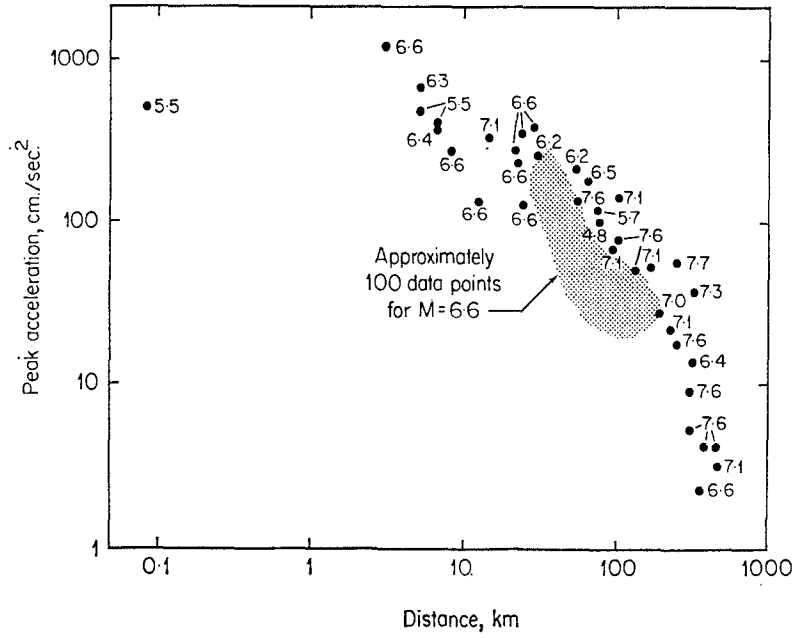


Figure 3. Attenuation of maximum acceleration

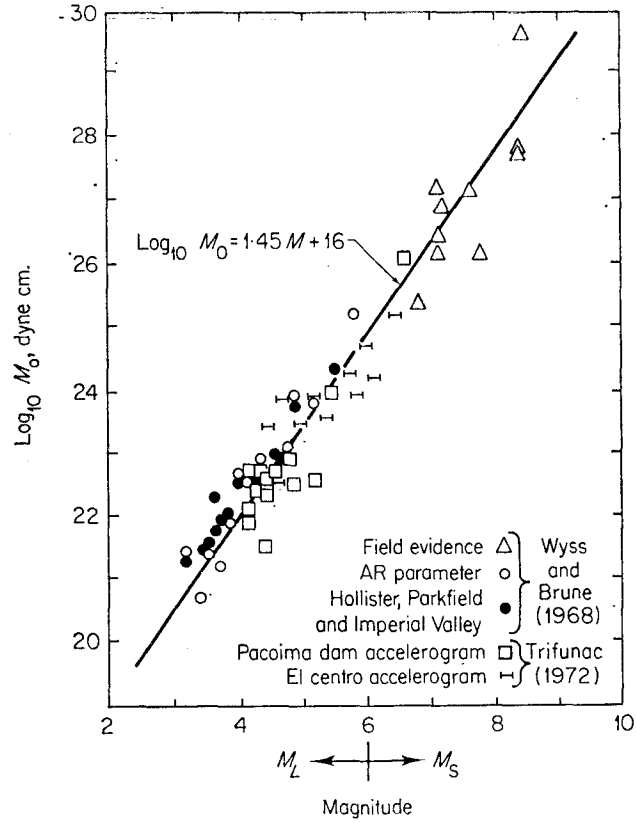


Figure 4. Logarithm of seismic moment as a function of magnitude

In engineering applications the so-called ‘pseudo relative velocity spectrum’, PSV, is often used in place of the relative velocity spectrum. It is equal to the product of the relative displacement spectrum, SD, and the natural frequency of the single degree of freedom system<sup>30</sup>

$$\text{PSV} \equiv \frac{2\pi}{T} \text{SD}$$

Similarly, the ‘pseudo absolute acceleration spectrum’ is defined by

$$\text{PSA} \equiv \left(\frac{2\pi}{T}\right)^2 \text{SD}$$

SD, PSV and PSA can be conveniently plotted on the common tripartite logarithmic plot versus logarithm of the period  $T$ .<sup>30</sup>

For a transient, band-limited, ground acceleration the amplitude of the high-frequency end of the SD spectrum tends to  $(T/2\pi)^2$  times the peak ground acceleration, while the long-period end of the SD spectrum tends to the maximum ground displacement. These properties of the SD spectrum are merely a consequence of the fact that the single degree of freedom system acts as an accelerometer for frequencies smaller than its natural frequency, and as a displacement meter for frequencies higher than its natural frequency. Thus, for example, depending on the importance of the structure, one may take the average or the maximum of the observed accelerations at a given distance (Figure 3) to find the high-frequency amplitude of the pseudo relative velocity spectrum. The long-period amplitude of the same spectrum would be  $2\pi\bar{u}/T$  for a station essentially at the fault. Using (10) and (15), for distances greater than about  $10r$ , this amplitude would become  $2\pi u_{\max}/T$  where

$$u_{\max} = \left(\frac{4}{7\pi}\right)^{\frac{1}{2}} \frac{1}{e} \frac{\sigma r^2}{\mu R} \quad (21)$$

Approximating the dislocation surface with a disc of radius  $r$  the moment  $M_0$  becomes<sup>14</sup>

$$M_0 = \frac{1}{7} \sigma r^3 \quad (22)$$

Combining (21), (22) and (20) we get

$$u_{\max} = \frac{1}{8e} \left(\frac{7}{\pi}\right)^{\frac{1}{2}} \frac{10^{1.45M+16.0}}{\mu r R} \quad (23)$$

Thus, at large distances, where only the dynamic field contributes to the ground displacement, (23) might be used to determine the approximate maximum of ground displacement associated with the  $S$ -wave motion. At intermediate distances,  $x \approx r$ , where all of the near, intermediate and far-field terms contribute to the maximum displacement amplitude, the long-period Fourier spectrum amplitudes of ground motion have a trend between  $\omega$  and  $\omega^2$  (Figure 2).

The above characterization of earthquake spectra, of course, gives only the general spectral trends for body waves in an elastic and homogeneous infinite space. Although this characterization may be used as the first order approximation of Fourier and response spectra of strong ground motion, it must be remembered that local geologic formations may change the spectral amplitudes appreciably through reflection, refraction, scattering and focusing effects,<sup>31,32</sup> and through the wave-guide phenomenon leading to surface waves.<sup>33</sup>

## CONCLUSIONS

The results of the foregoing analysis of the expected overall trends of the Fourier amplitude spectra of ground motion based on a simple dislocation model in an infinite elastic space can be summarized as follows:

1. The simplest physical characterization of the Fourier amplitude spectrum of strong ground motion is by two parameters: (a) the effective stress  $\sigma$  and (b) the seismic moment  $M_0$  for far-field motions, or the permanent static displacement  $u$  for near-field motions. The effective stress determines the high-frequency amplitude, while the seismic moment, or permanent static displacement, determines the long-period amplitude of the ground motion spectrum.

2. Recorded peak ground acceleration should be correlated with the effective stress of an earthquake since it is determined by the high-frequency end of the spectrum, and should not be correlated with earthquake magnitude. Peak acceleration can be used to determine the approximate high-frequency level of the response spectrum.

3. Since both earthquake magnitude and seismic moment are related to the long-period amplitude of the ground displacement spectrum, they can be related empirically by equation (20). Using equation (14) or (23), earthquake magnitude can be employed to determine approximately the long-period spectral amplitudes.

#### ACKNOWLEDGEMENTS

I wish to thank G. W. Housner and P. C. Jennings for critical reading of the manuscript and valuable suggestions. This research was supported by a grant from the National Science Foundation.

#### REFERENCES

1. R. W. Clough, 'Earthquake response of structures', Ch. 12 *Earthquake Engineering*, (Ed. R. L. Wiegel), Prentice-Hall, Englewood Cliffs, New Jersey, 1970.
2. M. D. Trifunac, 'A method for synthesizing realistic strong ground motion', *Bull. Seism. Soc. Am.* **61**, 1739-1753 (1971).
3. H. Benioff, 'The physical evaluation of seismic destructiveness', *Bull. Seism. Soc. Am.* **24**, 398-403 (1934).
4. M. A. Biot, 'A mechanical analyzer for the prediction of earthquake stresses', *Bull. Seism. Soc. Am.* **31**, 151-171 (1941).
5. J. L. Alford, G. W. Housner and R. R. Martel, 'Spectrum analysis of strong-motion earthquakes', Earthquake Eng. Res. Lab., California Institute of Technology, Pasadena, 1951.
6. D. E. Hudson, 'Some problems in the application of spectrum techniques to strong-motion earthquake analysis', *Bull. Seism. Soc. Am.* **52**, 417-430 (1962).
7. N. C. Nigam and P. C. Jennings, 'Calculation of response spectra from strong-motion earthquake records', *Bull. Seism. Soc. Am.* **59**, 909-922 (1969).
8. L. Zeevaert, 'Strong ground motions recorded during earthquakes of May 11th and 19th, 1969 in Mexico City', *Bull. Seism. Soc. Am.* **54**, 209-231 (1964).
9. G. W. Housner, 'Behavior of structures during earthquakes', *Proc. Am. Soc. Civ. Eng.* **85**, EM4, 109-129 (1959).
10. G. W. Housner, 'Design spectrum', Ch. 5 *Earthquake Engineering*, (Ed. R. L. Wiegel), Prentice-Hall, Englewood Cliffs, New Jersey, 1970.
11. A. S. Veletsos, N. M. Newmark and C. V. Chelapati, 'Deformation spectra for elastic and elastoplastic systems subjected to ground shock and earthquake motions', *3rd Wld Conf. Earthquake Engng II*, 663-680, New Zealand, 1965.
12. J. A. Blume, 'Earthquake ground motion and engineering procedures for important installations near active faults', *3rd Wld Conf. Earthquake Engng IV*, 53-69, New Zealand, 1965.
13. C. F. Richter, *Elementary Seismology*, Freeman & Co., San Francisco 1958.
14. J. N. Brune, 'Tectonic stress and the spectra of seismic shear waves', *J. Geophys. Res.* **75**, 4997-5009 (1970).
15. M. D. Trifunac, 'Stress estimates for the San Fernando, California, earthquake of February 9, 1971: main event and thirteen aftershocks', *Bull. Seism. Soc. Am.* **62**, 721-750 (1972).
16. A. T. Starr, 'Slip in a crystal and rupture in a solid due to shear', *Cambridge Phil. Soc. Proc.* **24**, 489-500 (1928).
17. L. Knopoff, 'Energy release in earthquakes', *Geophys. J.* **1**, 44-52 (1958).
18. V. I. Keilis-Borok, 'On estimation of the displacement in an earthquake source and of source dimensions', *Annali Geofisica*, **12**, 205-214 (1959).
19. F. C. Frank, 'Introduction to the discussion on source mechanisms', *Proc. VESIAC Conf.* Univ. of Michigan, Ann Arbor (1967).
20. T. Maruyama, 'On the force equivalent of dynamic elastic dislocations with reference to the earthquake mechanism', *Bull. Earthquake Res. Inst.*, Tokyo Univ. **41**, 467-486 (1963).
21. R. Burridge and L. Knopoff, 'Body force equivalents for seismic dislocations', *Bull. Seism. Soc. Am.* **54**, 1874-1888 (1964).
22. V. I. Keilis-Borok, 'Investigation of the mechanism of earthquakes', *Sov. Res. Geophys.* **4** (transl. *Tr. Geofiz. Inst.* **40**, 1957), Am. Geophys. U. Consultants Bureau, New York, 1960.
23. K. Aki, 'Generation and propagation of G waves from the Niigata earthquake of June 16, 1964, 2', *Bull. Earthquake Res. Inst.*, Tokyo Univ. **44**, 73-88 (1966).
24. M. D. Trifunac and J. N. Brune, 'Complexity of energy release from the Imperial Valley, California, Earthquake of 1940', *Bull. Seism. Soc. Am.* **60**, 137-160 (1970).
25. M. D. Trifunac, 'Tectonic stress and source mechanism of the Imperial Valley, California, Earthquake of 1940', *Bull. Seism. Soc. Am.* **62**, 1283-1302 (1972).
26. L. R. Sykes, 'Aftershock zones of great earthquakes, seismicity gaps, and earthquake prediction for Alaska and the Aleutians', *J. Geophys. Res.* **76**, 8021-8041 (1971).
27. J. N. Brune and C. R. Allen, 'A low-stress-drop, low-magnitude earthquake with surface faulting: The Imperial, California, Earthquake of March 4, 1966', *Bull. Seism. Soc. Am.* **57**, 501-514 (1967).
28. M. A. Chinnery, 'The strength of the earth's crust under horizontal shear stress', *J. Geophys. Res.* **69**, 2085-2089 (1964).
29. M. Wyss and J. N. Brune, 'Seismic moment, stress, and source dimensions for earthquakes in the California-Nevada region', *J. Geophys. Res.* **73**, 4681-4694 (1968).

30. D. E. Hudson, M. D. Trifunac and A. G. Brady, 'Strong motion accelerograms IIIA, response spectra', *Earthquake Eng. Res. Lab. EERL 72-80*, California Institute of Technology, Pasadena, 1972.
31. M. D. Trifunac, 'Surface motion on a semi-cylindrical alluvial valley for incident plane SH waves', *Bull. Seism. Soc. Am.* **61**, 1739-1753 (1971).
32. M. D. Trifunac, 'Scattering of plane SH waves by a semi-cylindrical canyon', *Int. J. Earthq. Engng Struct. Dyn.* **1**, 267-281 (1973).
33. M. D. Trifunac, 'Response envelope spectrum and interpretation of strong earthquake ground motion', *Bull. Seism. Soc. Am.* **61**, 343-356 (1971).